❷ Noonan 症候群における高度の側弯症

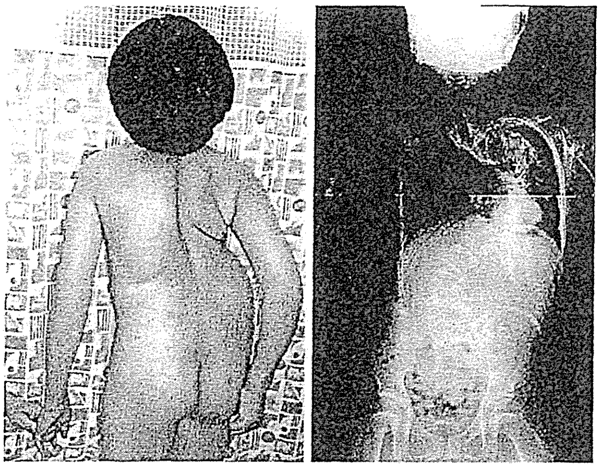

胸郭の著しい変形により肺野の圧迫が認められる.

は明らかではないが，椎体・靱帯・背筋の成長の問題があると考えられている.

- これらの疾患は，成長ホルモン治療の対象となる*3. 成長ホルモン治療により急激に身長が増加すると，側弯症が悪化することがある．側弯症がある場合はすべて治療を中止しなければならないわけではないが，十分に経過を観察し，悪化がみられるようであれば整形外科医と相談して中止を考慮する.

*3
Noonan 症候群では成長ホルモン分泌不全症を合併した場合に治療対象.

治療対象

- 側弯症は自然治癒することはないが，すべてが治療対象ではない.
- Cobb 角を計測し，20° 未満の軽度の側弯であれば経過を観察する.
- Cobb 角 30° 以上ではコルセットなど矯正具の適応となる*4. 体格と側弯部位に合わせた形状のものを作製して着用する.
- Cobb 角 40～50° 以上の高度の側弯では，胸郭の変形に伴う臓器障害の懸念もあるため，外科的治療が行われる（❷）．しかし，脊椎の手術は危険を伴うものであり，豊富な経験と高度の技術を有する施設を選択して行われるべきである.

*4
コルセット装着自体の有効性を疑問視する意見もある.

軟骨無形成症，軟骨低形成症

概念

- 軟骨細胞分化異常による内軟骨性骨化障害のため，長管骨の成長障害・頭蓋底の低形成による四肢短縮と特徴的顔貌をきたす疾患．骨系統疾患の一つで，以前は軟骨異栄養症と総称されていたが，現在は軟骨無形成症（achondroplasia），軟骨低形成症（hypochondroplasia）にほぼ統一されている．軟骨低形成症はより軽症.
- 発生頻度は，軟骨無形成症では 1 万出生に 1 人，軟骨低形成症は不明とされている.

❸ 軟骨無形成症の特徴的顔貌

前額突出，顔面中央部低形成，鞍鼻を認める．

❹ 軟骨無形成症の体格

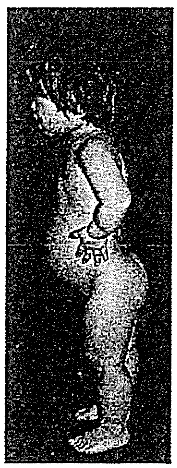

近位側優位の四肢の短縮，腰椎の前弯を認める．手指は三尖手の所見である．

❺ 軟骨無形成症の骨 X 線像（左手）

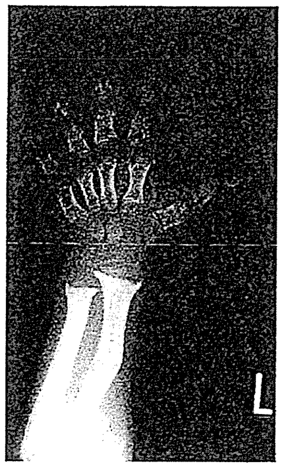

長管骨の形成不全と異形成が著明．

病因，病態

- 軟骨無形成症は，近位側に優位の四肢短縮，手指が短く三尖手とよばれる形態，腰椎前弯，O 脚のほか，前額突出，鞍鼻，顔面中央部低形成による特徴的顔貌を呈する（❸❹）．軟骨低形成症は，これらの所見がより軽度である．軟骨無形成症と低形成症の一部は *FGFR3* の遺伝子変異が病因であり，そのほとんどが G380R 変異である．常染色体優性遺伝の疾患である．

FGFR3：fibroblast growth factor receptor type 3（線維芽細胞増殖因子受容体 3 型）

- 軟骨無形成症では，成人になっても低身長にとどまり，男性 130 cm，女性 122 cm 程度である．
- 上気道の閉塞をきたしやすく睡眠時無呼吸の頻度が高い，中耳炎を起こしやすく，骨変形に伴った神経管の狭窄による神経障害をきたすこともある．
- 知能発達は正常であるが，体格のアンバランス（頭が大きく手足が短い）のため運動発達は障害されやすい．
- 大後頭孔狭窄により，水頭症，延髄の圧迫による呼吸中枢の障害と閉塞性呼吸障害をきたすこともある．これは突然死の原因ともなりうるため，注意を要する．

診断

- エコーの進歩により出生前診断が可能になり，胎内で四肢短縮に気づかれる場合も増加している．出生前に診断されても普通分娩にて出生し，周産期障害は伴わないことが多い．
- 軟骨無形成症は臨床所見から疑う．骨 X 線写真で臨床診断は確定する（❺）．新生児期から四肢の短縮と頭部が大きいアンバランスが明らかであるが，顔貌の特徴がはっきりしないこともある．骨 X 線写真でも特徴的所見が明らかでない場合もあり，注意を要する．
- 軟骨低形成症の診断は，新生児期には容易ではない．成長を観察し，成長

障害が明らかであれば骨X線写真で確認する．

- 最終的に確定診断は遺伝子検査で行う．軟骨低形成症はFGFR3の遺伝子変異をもたないものがある．

治療

- 日本では成長ホルモン治療が保険適用となっており，小児慢性特定疾患医療費助成の対象である．開始年齢は一応3歳以上となっている．成長ホルモンの治療効果は限られており，反応性にも個人差がある．予測身長から推測される治療効果は，軟骨無形成症で5～10cm程度の身長増加である．軟骨低形成症では反応性の良い例もある．
- 大後頭孔狭窄を有する場合，成長ホルモン治療が睡眠時無呼吸を悪化させることがあるので注意を要する．突然死の原因ともなりうる．
- 低身長に対する外科的治療として脚延長術がある．下腿と大腿，それぞれで10cmほどの伸長が可能とされ，計20cmの身長増加が見込まれる．しかし，大がかりな装置をつけ，入院も長期化するので本人への負担は大きい．

心理的な支援

- 知的発達は正常で，運動能力も体のバランスがとれるようになると個人差があるものの発達する．
- 普通学級を選択することには，本来支障はないはずであるが，学校の受け入れ体勢や級友の理解が得られないことがありうる．積極的に心理面での支援も行うとよい．学校生活においては，入学前にあらかじめ洗面所に踏み台を置くなど，自然な配慮を工夫する．

骨形成不全症

概念

- 骨形成不全症（OI）は，易骨折性を示す骨系統疾患である．発症頻度は2万出生に1人と考えられている．

OI：osteogenesis imperfecta

病型，病因

- 病型は，臨床像からSillenceにより4型に分類されていたが，近年Coleらが3つの型を追加し，I～VII型に分類し，さらに最近*LEPRE1*遺伝子変異によるVIII型の存在が提唱された（❻）．
- I～IV型において，I型コラーゲン遺伝子（*COL1A1*または*COL1A2*）の変異[*5]が認められ，この変異によるI型コラーゲンの量的・質的異常が骨脆弱性の原因と考えられている．I型コラーゲンは骨以外にも腱，靱帯，皮膚，強膜の重要な構造タンパクである．全体の約10％の患者では，別の遺伝子変異が疾患の原因と考えられている．
- cartilage-associated protein（CRTAP）は重症・致死性OIとVII型，FKBP10はIII型（組織はIV型），leprecan-like 1（LEPRE1）はVIII型において，責任遺伝子と考えられる．

*5
2種類のポリペプチド鎖3本がへリックス構造をつくり，それが重合してコラーゲン繊維となるが，*COL1A1*と*COL1A2*遺伝子に変異を有すると，この構造が崩れるために骨形成が量的に障害されたり，質的に脆弱であったりすると考えられる．

臨床所見

- 易骨折性・非典型的骨折，低身長，側弯，頭蓋底の変形とそれに伴う神経

❻ 骨形成不全症の病型と臨床像

型	遺伝形式	重症度	亜分類	骨折	骨変形	身長	子宮内死亡	強膜	歯牙	難聴
Ⅰ	AD	軽症	A	さまざま	通常ない	ほぼ正常	まれ	青色	正常	成人期50%
			B						形成不全	
		ⅠBより重症	C						正常	
Ⅱ	AD	周産期致死性	A	多数回の骨折，菲薄な頭蓋骨，扁平脊椎，長管骨アコーディオン変形	幅広い長管骨，数珠状肋骨	重度低身長	あり	濃い青色	?	?
			B		幅広い長管骨，正常肋骨					
			C		細い長管骨，細い数珠状肋骨					
			D		形態は保たれるが重度の骨萎縮．脊椎，骨盤は正常					
Ⅲ	ADまれにAR	重症		薄い肋骨，扁平脊椎，ガラス様骨，ポップコーン状骨端	中等症～重症	重度低身長	あり	青色	乳歯形成不全	しばしば
Ⅳ	AD	軽症～中等症	A	多発骨折	軽症～中等症	低身長	一部あり	正常～灰色	正常	時にあり
			B						形成不全	
Ⅴ	AD	中等症		多発骨折	中等症	さまざま	なし	正常	―	なし
Ⅵ	不明	中等症		多発骨折	四肢短縮	軽度低身長	なし	正常	―	なし
Ⅶ	AR	中等症		多発骨折	あり	軽度低身長	なし	正常	―	なし
Ⅷ	AR	重症～致死性		多発骨折	円形顔貌 短い樽状胸	重度低身長	あり	正常	―	―

AD：常染色体優性，AR：常染色体劣性．

❼ 骨形成不全症Ⅲ型の下肢骨X線像

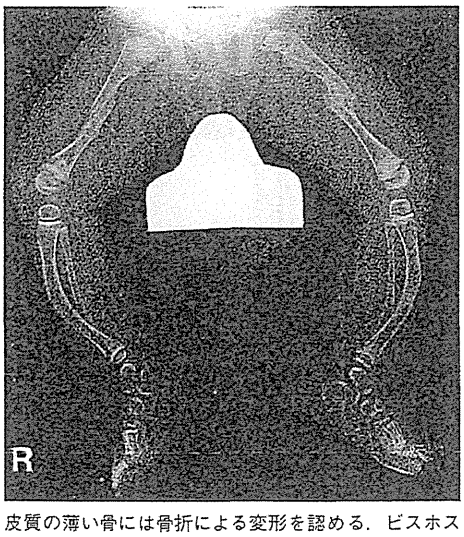

皮質の薄い骨には骨折による変形を認める．ビスホスホネート治療により歩行が可能となった．

管狭窄，青色強膜，難聴，歯牙形成不全，靭帯・皮膚の過伸展，頭蓋の虫食い状変化，紫斑がみられる．出現頻度や出現年齢は病型により異なる（❻）．

診断

- 基本的には臨床所見から診断される．検査所見では特異的なものはなく，血中・尿中Caの高値がみられる．骨X線写真は病型診断に有用である（❼）．可能であれば *COL1A1*，*COL1A2* の遺伝子診断を行う．

治療

- 治療の基本目標は，骨折とそれによる骨変形を避けることである．積極的なリハビリによる姿勢や運動の改善のほか，整形外科的に矯正骨切りや髄内釘固定を行うこともある．薬物治療としてビスホスホネートを使用する．
- 中等症～重症OI（Ⅲ，Ⅳ型）では，パミドロン酸二ナトリウム水和物（パミドロネート）（アレディア®）の点滴静注が最も一般的である．パミドロネートは年間の総投与量9mg/kgを超えない量とし，骨の代謝回転を考慮して1歳までは2か月に1回（各2日間），1歳以降は3か月に1回（各3日間）の点滴静注を行う．筆者は，入院の必要がない

よう，外来で月 1 回の点滴を行っている．初回投与時に，インフルエンザ様の発熱，CRP 上昇などがみられることがあるが，1 日で自然軽快する．血中 Ca が低下することがあり，とくに乳児でみられるので注意する．多くはとくに治療の必要はない．最近ではゾレドロネート（ゾメタ®）も使用されるようになり，パミドロネートより短時間の治療時間ですむ利点があるものの，使用経験数は未だ少ない．

- パミドロネートの骨塩量増加に対する有効性は，治療開始後 2 年（〜4 年）が最大で，その後は維持にとどまるとされている．治療中止時期についてはこれらのデータを元に個々の症例に応じ設定するのが実際的である．
- 軽症型に対する経口ビスホスホネートの有効性は議論があり，一定の結論をみていないが，自験例では思春期前男児において骨折数の有意な減少をみている．
- 低身長の改善と骨密度増加を目的として，成長ホルモン治療が試されているが，効果は明らかでない．

症例

症例 1　側弯症

18 歳，女性．成長ホルモン分泌不全症（中等症）あり，5 歳より成長ホルモン治療開始．8 歳ごろから側弯を認め，整形外科医に成長ホルモン治療の可否についてコンサルト，中止の必要はないとの判断で続行．側弯は経過観察の後コルセット着用，二次性徴の進行に伴い側弯の進行を認め成長ホルモンは中止とした．15 歳時，整形外科にて外科的修復術施行．手術により身長は＋6 cm の改善をみた．整形外科医より骨端線未閉鎖のため成長ホルモン再開を促され，骨年齢は J-RUS 法により 12 歳と進行していたが再開，＋3 cm の身長増加を認めた．

症例 2　軟骨無形成症

6 歳，女児．低身長を主訴に来院．特徴的身体所見と骨所見，遺伝子検査にて *FGFR3* の G380R 変異を認め軟骨無形成症と診断．3 歳より成長ホルモン治療開始．比較的反応は良好で，標準成長曲線に沿って成長している（通常は年齢とともに標準から離れていく）．

症例 3　骨形成不全症

3 歳，男児．OI Ⅲ 型にて新生児期は胸郭低形成による呼吸不全あり，4 か月間 NICU に入院していた．退院後すぐに OI 治療目的にて当科受診．それまでに骨折歴 6 回，大腿，下腿と上腕に骨折後の変形を認めた．退院後 6 か月よりパミドロネート月 1 回外来での点滴治療（0.75 mg/kg/回×12 回/年）を開始．2 年 6 か月を経て，骨密度の上昇・骨折数の減少に加え，歩行が可能となり，O 脚が悪化しないよう工夫が必要であるが，リハビリに通いながら歩行訓練を行っている．

IV-2.　研究成果の刊行物・別刷

（平成 24 年度）

中枢性摂食異常症

飢餓応答の分子機構と中枢性摂食異常症

亀井康富*1　田中　都*2　菅波孝祥*3
小川佳宏**2

要　旨

中枢性摂食異常症における極端なダイエットによる飢餓状態は，著しい骨格筋萎縮とQOLの低下をもたらす．一方，飢餓時には免疫機能が低下することが知られる．本稿では，中枢性摂食異常症において認められる全身の飢餓応答として，① 飢餓における骨格筋代謝と骨格筋萎縮に関連する遺伝子発現制御，② 飢餓における免疫機能障害として骨髄B細胞分化異常の分子機構について概説し，我々の研究成果を紹介する．

はじめに
－飢餓と中枢性摂食異常症－

中枢性摂食異常症の中でもやせを主体とする神経性食欲不振症（拒食症）では，身体的な栄養障害（飢餓状態）を呈することにより，重症例では体力や筋力の低下によって転倒しやすくなり，運動や日常生活が困難となる．また，白血球減少，貧血，血小板減少などとともに免疫機能の低下が観察される．以上のように，中枢性摂食異常症の病態は飢餓や低栄養と密接に関連している[1~3]．本稿では飢餓における骨格筋代謝障害と免疫機能障害の分子機構について，我々の最近の研究結果を概説する．

*1 東京医科歯科大学大学院医歯学総合研究科
臓器代謝ネットワーク講座　特任教授
*2 同　分子内分泌代謝学分野（糖尿病・内分泌・代謝内科）**2 同　教授
*3 東京医科歯科大学難治疾患研究所
分子代謝医学研究室　准教授

キーワード：飢餓，神経性食欲不振症，骨格筋，レプチン

飢餓における生体の代謝変動

飢餓による栄養の環境変化に対して，全身臓器においてエネルギー代謝を変化させることにより適応する[4]．絶食により，まず肝臓のグリコーゲンが消費される．骨格筋では，飽食時にはグルコースと脂質がエネルギー源として利用されるが，絶食時には血糖値の低下を防ぐためにエネルギー源をグルコースから脂質へとシフトする．脂肪組織では，トリグリセリドが分解されて遊離脂肪酸とグリセロールに変換され，遊離脂肪酸は骨格筋においてβ酸化によってエネルギー源となり，グリセロールは肝臓において糖新生に利用される．長期間の飢餓においては，骨格筋ではアクチンやミオシンなどの構造タンパク質が分解され，アミノ酸は肝臓にて糖新生の材料として利用される[5]．以上のように，飢餓時に

図1　飢餓時の生体の代謝変動の概要

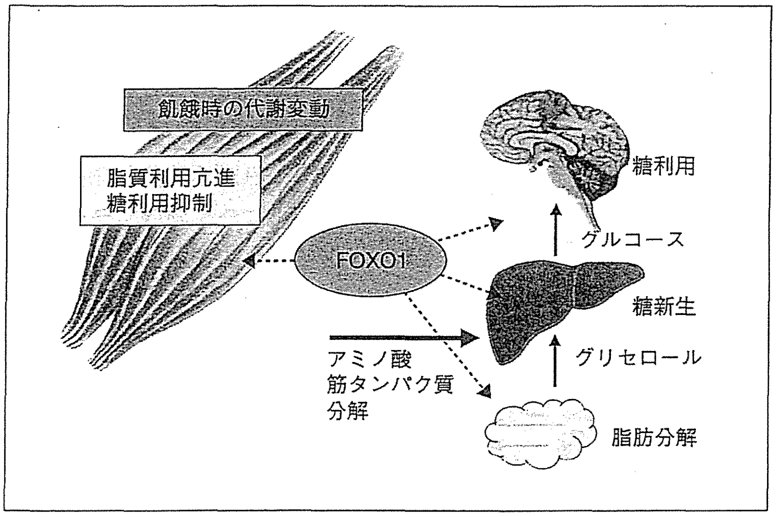

飢餓による栄養状態の変化に対して，全身の臓器においてエネルギー代謝を変化させて適応する．脂肪組織においてはトリグリセリドが分解されて遊離脂肪酸とグリセロールに変換され，グリセロールは肝臓において糖新生に利用される．同様に骨格筋ではアクチンやミオシンなどの構造タンパク質が分解され，アミノ酸は肝臓において糖新生に利用される．以上のように，飢餓時には脳が低血糖状態にならないように複数の組織で合目的に代謝調節されている．転写調節因子 FOXO1 は，飢餓に応答して骨格筋で多くの標的遺伝子を発現調節する．

は脳が低血糖状態にならないように複数の臓器で合目的に代謝調節されている（図1）．

飢餓における骨格筋代謝とフォークヘッド型転写調節因子 FOXO1

Forkhead box protein–O1（FOXO1）はフォークヘッド型の転写調節因子であり，同化ホルモンであるインスリンに拮抗することが知られている．従来，絶食時の肝臓において，FOXO1 は糖新生の主要な酵素であるグルコース6ホスファターゼ（G6Pase）やホスホエノールピルビン酸カルボキシキナーゼ（PEPCK）の遺伝子発現を活性化することが報告されてきた[6]．我々はすでに，飢餓（絶食）により骨格筋における FOXO1 の遺伝子発現が増加することを踏まえて，骨格筋特異的に FOXO1 を過剰発現するトランスジェニックマウスを作出し，FOXO1 が骨格筋量と赤筋線維の遺伝子発現を負に制御することを証明した[7]．従来，骨格筋における FOXO1 の標的遺伝子が複数同定されている．例えば C2C12 筋培養細胞で，FOXO1 は脂質の取り込みに関与するリポタンパク質リパーゼ（LPL）の遺伝子発現を活性化する[8]．また，解糖系の反応を抑制するピルビン酸脱水素酵素キナーゼ4（PDK4）が，FOXO1 により活性化されることが報告されている[9]．我々は最近，絶食後の再摂食時に骨格筋において，核内受容体 RXRγ/LXR によって脂質合成のマスターレギュレーターである SREBP1c の遺伝子発現が著しく増加すること，これが FOXO1 によって抑制されることを見いだした[10]．さらに，脂肪組織では FOXO1 がトリグリセリド分解酵素 ATGL 遺伝子を活性化して脂肪分解が促進され，脂質がエネルギーとして利用されるようになる[11]．以上の変化

図2　レプチンの免疫機能調節作用

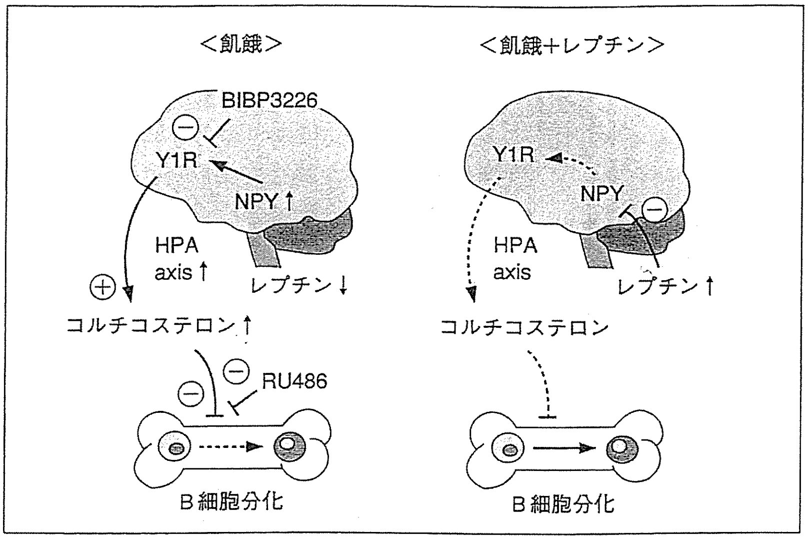

レプチンは栄養状態に応じて脂肪組織より産生・分泌され，主に視床下部に発現するレプチン受容体を介して摂食やエネルギー調節に関与することが知られている．レプチンは炎症反応や免疫機能も制御すること，その少なくとも一部は中枢神経系を介することが証明されている[18)19)]．絶食下では，脳内レプチンシグナルの欠損により視床下部の摂食促進神経ペプチドNPY-Y1受容体経路が活性化されてコルチコステロン産生が増加し，骨髄B細胞分化異常がもたらされるが，脳室内レプチンの補充によって抑制される（HPA axis：視床下部－下垂体－副腎軸）．
BIBP3226：NPY-Y1受容体拮抗薬，RU486：コルチコステロン拮抗薬

は，短期間の絶食では生体のエネルギー源として骨格筋における糖利用が抑制され，脂質利用が促進されるという生理的反応と合致するものである（図1）．

FOXO1あるいはそのホモログであるFOXO3によって骨格筋特異的ユビキチンリガーゼであるatrogin1遺伝子が活性化されること，オートファジーに重要なLC3b，Gabarapl1，Atg12lなどの遺伝子が活性化されてタンパク質分解が促進されることが明らかにされている[12)]．我々は，FOXO1マウスの骨格筋ではリソソームに存在するタンパク質分解酵素カテプシンLの発現が増加すること，FOXO1がカテプシンL遺伝子のプロモーター上ではFOXO1の結合配列にリクルートされることを証明した[13)]．以上の成績より，長期間の絶食（飢餓）では，骨格筋萎縮に伴って分解された骨格筋タンパク質由来のアミノ酸は肝糖新生によって糖に変換され，脳におけるエネルギー源として供給されるのである（図1）．

FOXO1は肝臓や骨格筋のみならず視床下部において，摂食促進神経ペプチドAgrp遺伝子を活性化して摂食抑制神経ペプチドPomc遺伝子を抑制し，絶食時に摂食行動を促進させる[14)]．すなわち，FOXO1は飢餓時の生理的適応のために，複数の臓器において合目的に代謝関連遺伝子を発現調節すると考えられる．

飢餓における免疫機能障害

肥満や栄養飢餓状態において，生体の栄養状態を感知して免疫応答を制御する分子機構には不明な点が多い．レプチンは脂肪細胞か

ら分泌される代表的なアディポサイトカインであり，体脂肪量に比例して産生が増加し，食欲やエネルギー代謝調節に関与する[15]．一方，神経性食欲不振症では，体脂肪量の減少を反映して血中レプチン濃度が著しく低下する．神経性食欲不振症において認められる性腺ホルモンの低下やコルチゾールの増加などの内分泌代謝障害に，減少するレプチンの関与が示唆される．実際，実験動物を用いた検討により，絶食時にはヒトの神経性食欲不振症と同様に内分泌代謝機能あるいは免疫機能が大きく変化するが，レプチンの補充によってその一部が抑制されることが報告されている．一方，血中レプチン濃度が著しく低下した絶食マウスでは胸腺の萎縮やＴ細胞数の低下が認められるが，レプチンの末梢投与により改善する[16]．また，レプチンを欠損する遺伝性肥満 *ob/ob* マウスにおいても同様の変化が認められる[17]．すなわち，絶食によりもたらされる身体機能の変化には，栄養状態の悪化による変化とレプチンの低下により生じる変化があると考えられる．

骨髄Ｂ細胞分化とレプチン

我々は最近，飢餓時におけるレプチンの病態生理的意義を明らかにする目的で，免疫系，特に骨髄におけるＢ細胞分化を検討し，絶食により血中レプチン濃度の低下と骨髄Ｂ細胞の分化異常が認められること，レプチンを補充することによりＢ細胞の分化異常が回復することを見いだした[18]．一方 *ob/ob* マウスでは，過食による肥満や高血糖など絶食マウスとは逆の表現型を呈するにもかかわらず，絶食と同様の骨髄Ｂ細胞分化異常が認められた．さらに，ごく少量のレプチンを脳室内に補充することにより，絶食マウスや *ob/ob* マウスにおいて認められる骨髄Ｂ細胞分化異常はほぼ完全に回復することが明らかになった．グルココルチコイド受容体拮抗薬の投与により，絶食による骨髄Ｂ細胞分化障害が抑制されること，摂食促進神経ペプチド（ニューロペプチドＹ：NPY–Y1）受容体拮抗薬の脳室内投与により，絶食による血中コルチコステロン濃度上昇の抑制と骨髄Ｂ細胞分化障害が抑制されたことより，レプチンのＢ細胞分化制御作用には，絶食時における脳内レプチンシグナルの欠損による視床下部－下垂体－副腎系の活性化が関与することが示唆された．すなわち，脂肪組織由来ホルモンであるレプチンが生理的な骨髄Ｂ細胞分化に重要な役割を果たすことが示唆された．以上より，中枢神経系を介するレプチンの免疫調節作用が示唆された（図２）[18]．

おわりに

絶食や極端なダイエットにより誘導される骨格筋の量的・質的な変化や免疫応答の変化の分子機構の解明は，中枢性摂食異常症の病態の理解に繋がると考えられる．今後，中枢性摂食異常症において認められる骨格筋萎縮や免疫力低下の新しい予防法・治療法の確立が期待される．

文　　献

1) 公益財団法人難病医学研究財団難病情報センターホームページ: 厚生労働省難治性疾患克服研究事業 (臨床調査研究分野) 対象疾患. http://www.nanbyou.or.jp/entry/149
2) 堀川玲子: 神経性食欲不振症の病態－内分泌障害・骨粗鬆症など. アディポサイエンス 7 (3): 256–262, 2011.
3) 鈴木(堀田)眞理: 中枢性摂食異常症 わが国の現状と問題点. Pharma Medica 27 (10): 53–56, 2009.
4) Salway J G: Metabolism at a glance. Second Edition. Blackwell Science Ltd., London, 1999.
5) 矢ヶ崎一三, 他: アミノ酸の機能特性. 日本栄養食糧学会, 建帛社, 2007.
6) Nakae J, et al: The forkhead transcription factor Foxo1 (Fkhr) confers insulin sensitivity onto glucose–6–phosphatase expression.

J Clin Invest 108 (9): 1359–1367, 2001.
7) Kamei Y, et al: Skeletal muscle FOXO1 (FKHR) transgenic mice have less skeletal muscle mass, down–regulated type I (slow twitch/red muscle) fiber genes, and impaired glycemic control. J Biol Chem 279 (39): 41114–41123, 2004.
8) Kamei Y, et al: A forkhead transcription factor FKHR up–regulates lipoprotein lipase expression in skeletal muscle. FEBS Lett 536 (1–3): 232–236, 2003.
9) Furuyama T, et al: Forkhead transcription factor FOXO1 (FKHR)–dependent induction of PDK4 gene expression in skeletal muscle during energy deprivation. Biochem J 375 (Pt 2): 365–371, 2003.
10) Kamei Y, et al: Regulation of SREBP1c gene expression in skeletal muscle: role of retinoid X receptor/liver X receptor and forkhead–O1 transcription factor. Endocrinology 149 (5): 2293–2305, 2008.
11) Chakrabarti P, et al: FoxO1 controls insulin–dependent adipose triglyceride lipase (ATGL) expression and lipolysis in adipocytes. J Biol Chem 284 (20): 13296–13300, 2009.
12) Zhao J, et al: FoxO3 coordinately activates protein degradation by the autophagic/lysosomal and proteasomal pathways in atrophying muscle cells. Cell Metab 6 (6): 472–483, 2007.
13) Yamazaki Y, et al: The cathepsin L gene is a direct target of FOXO1 in skeletal muscle. Biochem J 427 (1): 171–178, 2010.
14) Kitamura T, et al: Forkhead protein FoxO1 mediates Agrp–dependent effects of leptin on food intake. Nat Med 12 (5): 534–540, 2006.
15) Ogawa Y, et al: Increased glucose metabolism and insulin sensitivity in transgenic skinny mice overexpressing leptin. Diabetes 48 (9): 1822–1829, 1999.
16) Lord G M, et al: Leptin modulates the T–cell immune response and reverses starvation–induced immunosuppression. Nature 394 (6696): 897–901, 1998.
17) Howard J K, et al: Leptin protects mice from starvation–induced lymphoid atrophy and increases thymic cellularity in ob/ob mice. J Clin Invest 104 (8): 1051–1059, 1999.
18) Tanaka M, et al: Role of central leptin signaling in the starvation–induced alteration of B–cell development. J Neurosci 31 (23): 8373–8380, 2011.
19) Tanaka M, et al: Role of central leptin signaling in renal macrophage infiltration. Endocr J 57 (1): 61–72, 2010.

Molecular Mechanisms in Starvation Response and Anorexia Nervosa

Yasutomi Kamei[1], Miyako Tanaka[2], Takayoshi Suganami[3], Yoshihiro Ogawa[2]

[1] Department of Organ Network and Metabolism, Graduate School of Medical and Dental Sciences, Tokyo Medical and Dental University
[2] Department of Molecular Endocrinology and Metabolism, Graduate School of Medical and Dental Sciences, Tokyo Medical and Dental University
[3] Department of Molecular Medicine and Metabolism, Medical Research Institute, Tokyo Medical and Dental University

Am J Physiol Endocrinol Metab 302: E781–E787, 2012.
First published January 17, 2012; doi:10.1152/ajpendo.00616.2011.

Increased expression of miR-325-3p by urocortin 2 and its involvement in stress-induced suppression of LH secretion in rat pituitary

Takahiro Nemoto, Asuka Mano, and Tamotsu Shibasaki

Department of Physiology, Nippon Medical School, Tokyo, Japan

Submitted 2 December 2011; accepted in final form 13 January 2012

Nemoto T, Mano A, Shibasaki T. Increased expression of miR-325-3p by urocortin 2 and its involvement in stress-induced suppression of LH secretion in rat pituitary. *Am J Physiol Endocrinol Metab* 302: E781–E787, 2012. First published January 17, 2012; doi:10.1152/ajpendo.00616.2011.—Urocortin 2 (Ucn2) is a member of the corticotropin releasing factor (CRF) peptide family, which binds to CRF type 2 receptor. We previously reported on expression of Ucn2 in proopiomelanocortin cells of rat pituitary and its inhibitory action on LH secretion. We also demonstrated that Ucn2 is involved in the mechanism underlying immobilization-induced suppression of LH secretion; the details remain unclear. Here, we found that Ucn2 increased the expression of miR-325-3p, one of three microRNAs with predicted sequence for binding to LH β-subunit 3′-untranslated region (3′-UTR) in monolayer cultured rat anterior pituitary cells, and that miR-325-3p was expressed in LH cells of the anterior pituitary. Immobilization also increased miR-325-3p expression in the anterior pituitary, and its increase was blocked by pretreatment with anti-Ucn2 IgG. Overexpression of miR-325-3p in cultured pituitary cells significantly suppressed intracellular contents and secretion of LH, while miR-325-3p knockdown blocked Ucn2-induced suppression of intracellular contents and secretion of LH. Coexpression of miR-325-3p with LH β-subunit 3′-UTR-fused luciferase vector significantly suppressed luciferase activity compared with that of mock transfectants. These results suggest that miR-325-3p is involved in immobilization-induced suppression of LH translation and secretion and that Ucn2 plays a role in the increase in miR-325-3p expression.

luteinizing hormone; microRNA; stress

REPRODUCTIVE FUNCTION IS SUPPRESSED by corticotropin-releasing factor (CRF), adrenocorticotropin, β-endorphin, and glucocorticoids, composing the hypothalamic-pituitary-adrenal axis under stress exposure (28, 29). We previously demonstrated that urocortin 2 (Ucn2), a member of the CRF peptide family (27), is expressed in proopiomelanocortin (POMC) cells of the anterior and intermediate lobes of the rat pituitary (32) and that in both sites CRF increases its mRNA expression (20). We also reported that Ucn2 suppresses luteinizing hormone (LH) secretion without influencing LH β-subunit mRNA expression, whereas a selective CRF type 2 receptor (CRF-R2) antagonist and a specific siRNA against CRF-R2 significantly increase LH secretion and LH β-subunit mRNA expression in monolayer cultured anterior pituitary cells of rats (23). A possible explanation for the inconsistency of effects between Ucn2 and its blockades on LH β-subunit mRNA expression is proposed; the expression level of LH β-subunit mRNA is already suppressed by endogenous Ucn2 secreted by POMC cells into the culture medium, and exogenous Ucn2 could not induce further suppression of LH β-subunit mRNA expression (6). Furthermore, we have shown that anti-Ucn2 IgG partially blocks immobilization-induced suppression of LH secretion and LH β-subunit mRNA expression (21). Considered together, these findings suggest that pituitary Ucn2 inhibits LH secretion and LH β-subunit mRNA expression and is involved in immobilization-induced suppression of reproductive function, although the details of the mechanism remain unclear.

Glycoprotein hormones such as LH, follicle-stimulating hormone (FSH), thyroid-stimulating hormone, and human chorionic gonadotropin are members of a family of cysteine-rich proteins, each consisting of α- and β-subunits; the α-subunit is common to all, and the β-subunit confers specificity (26). Expression of gonadtropins is regulated by positive and negative feedback mechanisms (25). Sex steroid hormones control the synthesis of each subunit separately but in a coordinated fashion (10). Regulation of transcription and translation differs for LH and FSH: inhibin-induced inhibition of SMAD signaling prevents activation of the FSH but not the LH β-subunit promoter (8). Regulatory mechanisms involved in the posttranscriptional and translational processes during LH β-subunit synthesis, especially their suppressive mechanisms, are unclear at present.

MicroRNAs (miRNAs) are short RNA molecules, ~22 nucleotides long on average, that are found in most types of eukaryotic cells (3). They are posttranscriptional regulators that usually induce translational repression and gene silencing in animals after binding to complementary sequences on target mRNAs. To the best of our knowledge, there have been no previous reports of the involvement of miRNAs in the regulation of pituitary hormone secretion. We hypothesized that Ucn2 might induce expression of miRNAs, which may then be involved in stress-induced suppression of LH secretion. To test this hypothesis, through database searches, we identified miRNAs predicted to bind to the LH β-subunit 3′-UTR, determined their expression levels in the Ucn2-treated monolayer cultured anterior pituitary cells of rats and pituitaries of immobilization-exposed rats, and then assessed the effects of miRNA overexpression and knockdown on LH β-subunit mRNA expression, intracellular LH content, and LH secretion.

MATERIALS AND METHODS

Animals. Six- and seven-week-old male Wistar rats were maintained at 23 ± 2°C in a 12:12-h light-dark cycle (lights on at 0800, off at 2000). They were allowed ad libitum access to laboratory chow and distilled water. All experimental procedures were reviewed and approved by the Laboratory Animals Ethics Review Committee of Nippon Medical School.

Primary culture of pituitary cells. Thirty male rats (6 wk old) were killed by decapitation, and their pituitary glands were removed under sterile conditions. The anterior pituitary lobes were collected, pooled together, and then mechanoenzymatically dispersed as previously

Address for reprint requests and other correspondence: T. Nemoto, Dept. of Physiology, Nippon Medical School, 1-1-5 Sendagi, Bunkyo-ku, Tokyo, 113-8602 Japan (E-mail: taknemo@nms.ac.jp).

described (20), but with several modifications. Briefly, lobes were washed twice in PBS and then incubated at room temperature in the PBS containing 0.01% dispase (Godoshusei, Tokyo, Japan) with constant stirring for 30 min. After washing with PBS three times, cells were plated in 24-well plates or 60-mm dishes and cultured with 10% FBS containing DMEM-F10 HAM culture medium (Sigma-Aldrich, St. Louis, MO) supplemented with an antibiotics/antimyotic solution (GIBCO, Auckland, NZ). The cells were subsequently allowed to attach to the plating surfaces at 37°C in a humidified 5% CO_2-95% air incubator for 4 days. On the day of experiment, the culture media were changed. Cells were treated with Ucn2 at concentrations of 1, 10, 30, and 100 pM for 1 h or 100 pM Ucn2 for 0.5, 1, and 2 h. After incubations, the cells were assayed for miRNA expression.

Passive immunization. We previously generated antisera against mouse Ucn2 (32). The IgG fraction was purified from serum obtained after the fifth booster by using a protein A-sepharose column. The specificity of this antiserum to Ucn2 was described in our previous reports (32). Cross-reactivities of the antiserum with rat Ucn2, rat CRF, Ucn1, and Ucn3 were 83.3, 0.0, 0.014, and 0.023%, respectively. Twenty male rats were administrated antiserum IgG to Ucn2 or normal rabbit serum (NRS) IgG (1 mg/kg body wt ip) dissolved in 1 ml normal saline. Two hours later, they were exposed to 90 min of immobilization stress (21). Rats were then killed immediately, and their trunk blood and pituitaries were collected. Trunk blood was placed into tubes containing EDTA-2Na (1 mg/ml blood) and centrifuged at 3,000 rpm for 20 min at 4°C. One-milliliter aliquots were transferred into 1.5-ml Eppendorf tubes and store at −80°C until use.

Stress exposure. Twenty male rats (7 wk old) were wrapped in a flexible wire mesh and kept for 90 min between 1300 and 1500 in an isolated room (1, 21). Rats were killed in the adjacent room immediately after immobilization, and their pituitaries were collected for RNA expression analysis. Nonstressed control rats were housed in a separate room from the stressed rats and were otherwise treated the same way.

miRNA identification. The miRBase (www.mirbase.org) and TargetScan (www.targetscan.org) database were searched for miRNAs predicted to bind to the LH β-subunit 3′-UTR.

In situ hybridization and immunohistochemistry. Digoxigenin-labeled LNA probe against mmu-miR-325-3p was purchased from Exiqon (Woburn, MA). Pituitaries were cryosectioned, dried for 30 min, and then fixed in 4% paraformaldehyde. Sections were permeabilized by proteinase K (10 μg/ml) for 10 min at 37°C and postfixed with 4% paraformaldehyde at 4°C. Prior to prehybridization, sections were acetylated in 0.25% acetic anhydride and 1.16% triethanolamine (Wako Pure Chemicals, Tokyo, Japan). Sections were prehybridized for 60 min in 50% formamide hybridization buffer, and then the sections were hybridized with denatured probe in 50% formamide hybridization buffer at 55°C overnight. The slides were washed in decreasing salt solutions (4×, 2×, and 0.5× saline sodium citrate). Signals were detected by anti-DIG-alkaline phosphatase conjugate (Roche Diagnostics, Mannheim, Germany) followed by detection with nitroblue tetrazolium/5-bromo-4-chloro-3-indolyl phosphate (Roche Diagnostics).

Upon completion of the chromogen reaction, slides were treated in 0.3% H_2O_2 for 30 min at room temperature, and the sections were incubated in 10% normal goat serum for 20 min and then incubated for 60 min at room temperature with an antibody to LH (1:5,000 dilution; Chemicon, Temecula, CA). Sections were incubated for 30 min with a secondary biotinylated goat anti-rabbit IgG (1:200 dilution; Vector Laboratories, Burlingame, CA). Sections were then incubated with an avidin-biotin-peroxidase complex (Vector Laboratories) for 30 min at room temperature, and the antibody-peroxidase complex was visualized using a Vector DAB kit (Vector Laboratories). When the staining had reached appropriate intensity, the tissue was rinsed in PBS, dehydrated through graded alcohols, cleared in xylenes, and coverslipped with VectaMount (Vector Laboratories). Images were captured with a microscope (AX-80; Olympus, Tokyo, Japan) using a color digital camera (DP72, Olympus) and digitized by an image analysis system (cellSens software, Olympus).

Transfection and Ucn2 treatment. miRNA overexpression vectors pBA-miR-325-3p and pBA-mock, and miRNA knockdown vectors pDecoy-miR-325-3p and pDecoy-mock were purchased from Takara Bio (Shiga, Japan). Each plasmid (2.5 μg) was cotransfected into primary pituitary cells with pAcGFP vector (2.5 μg) to validate the success of the transfection using Multifectam (Promega, Madison, WI) according to the manufacturer's instructions. After 72 h, culture medium was changed to fresh DMEM-F10 HAM medium containing Ucn2 at a concentration of 100 pM and then incubated for 1 h. To check whether the plasmids were successfully transfected into the cells, GFP fluorescence was assessed 48–72 h after transfection under fluorescent microscope.

Hormone assay. Frozen 1-ml aliquots of plasma or culture medium were thawed and LH concentrations measured using a rodent LH ELISA test (ERKR7010; Endocrine Technologies, Newark, NJ) according to the manufacturers' instructions. Literature supplied with the kit indicated 0.5 ng/ml as the assay sensitivity.

RNA extraction and real-time RT-PCR analysis. Total RNA was extracted from cultured pituitary cells and rat pituitaries using RNAiso Plus (Takara). For miRNA expression analysis, first-strand cDNA was synthesized using 1 μg of denatured total RNA at 37°C for 1 h and then terminated at 85°C for 5 min using Mir-X miRNA First-Strand Synthesis and SYBR qRT-PCR kits (Clontech Laboratories, Mountain View, CA). For mRNA expression analysis, first-strand cDNA was generated using 0.5 μg of denatured total RNA at 37°C for 15 min, 84°C for 5 s, and 4°C for 5 min using a PrimeScript RT reagent kit with gDNA Eraser (Takara). PCR was performed by denaturation at 94°C for 5 s and annealing-extension at 60°C for 30 s for 40 cycles using SYBR premix Ex Taq (Takara) and specific primers for rat LH β-subunit and GAPDH, as previously reported (21). To normalize each sample for RNA content, GAPDH, a housekeeping gene, or U6 small nuclear RNA (Clontech) were used for mRNA and miRNA expression analyses, respectively. Diluted normal rat pituitary cDNA and the second-derivative method were used as the standard and for calculating C_T values, respectively (24).

Northern blotting of miRNA. Total RNA from transfectants was separated by electrophoresis in 15% acrylamide gel containing 8 M urea. RNA was then electrically transferred to nylon membranes and fixed by UV cross-linking, prehybridized with DIG Easy Hyb solution (Roche Diagnostics) containing 10 μg/ml yeast tRNA at 45°C for 1 h, and then hybridized with 3′-DIG-labeled miRCURY LNA miRNA detection probe against mmu-miR-325-3p (Exiqon) at 45°C for 14 h. Signals were detected with a DIG luminescent detection kit according to the manufacturer's instructions (Roche Diagnostics).

3′-UTR assay. Synthetic oligonucleotide for LH β-subunit 3′-UTR, positioned from translational termination codon together with *Nhe*I and *Xho*I linker at its 5′ and 3′ end, respectively, and its antisense oligonucleotide were synthesized by Invitrogen (Carlsbad, CA). Oligonucleotides were annealed, digested with *Nhe*I and *Xho*I, and then the *Nhe*I-*Xho*I fragment was subcloned into *Nhe*I and *Xho*I sites of pmir-Glo plasmid [Promega, Madison, WI; pmir-Glo-LHβ 3′-UTR (WT); see Fig. 5*A*] (30). We also generated a 3′-UTR variant that was not recognized by miR-325-3p [pmir-Glo-LHβ 3′-UTR (SC); see Fig. 5*A*]. pmir-Glo-LHβ 3′-UTR (WT), pmir-Glo-LHβ 3′-UTR (SC), or pmir-Glo-mock plasmid and pBA-miR-325-3p or pBA-mock plasmid (2.5 μg of each plasmid amount) were cotransfected with Multifectam (Promega) into HEK293 cells and seeded in 60-mm dishes. Cells were collected after 72 h and assayed using the dual-luciferase reporter assay system according to the manufacturer's instructions (Promega).

Statistical analysis. Statistical analysis was performed by ANOVA followed by Tukey's post hoc test using Prism 5.0 software (GraphPad Software, La Jolla, CA). Pituitary cell culture using the same experimental protocol was performed twice. For real-time RT-PCR data, all results were expressed as percentage of control values. Statistical significance was defined at the $P < 0.05$ level.

RESULTS

Ucn2 increases miRNA expression in monolayer cultured rat pituitary cells. A search of miRNA databases revealed three miRNAs, rno-miR-325-3p (MI0000596), rno-miR-370 (MI0003486), and rno-miR-742 (MI0006161), with sequences predicted for binding to positions 59–65, 34–40, and 66–71 of LH β-subunit 3′-UTR, respectively (Fig. 1*A*). miR-325-3p appears to be present in essentially all pituitary cells, including those that are immunopostive for LH by a double-labeling technique for combined in situ hybridization and immunohistochemical analysis (Fig. 1*B*). Treatment of monolayer cultured rat anterior pituitary cells with Ucn2 significantly increased miR-325-3p expression, whereas there was no change in miR-370 and miR-742 levels (data not shown). Treatment with Ucn2 for 1 h significantly increased miR-325-3p expression at concentrations of 30 pM (1.75 ± 0.16-fold vs. control) and 100 pM (2.41 ± 0.15-fold vs. control) (Fig. 2*A*). A time course study revealed that miR-325-3p expression was significantly increased 0.5, 1, and 2 h (1.79 ± 0.18-, 2.41 ± 0.16-, and 1.59 ± 0.12-fold vs. control, respectively) after treatment with Ucn2 at a concentration of 100 pM (Fig. 2*B*).

Immobilization stress increases mir-325-3p expression, and anti-Ucn2 IgG blocks the increase in the pituitary. Ninety-minute immobilization stress significantly increased miR-325-3p expression in the anterior pituitary of rats pretreated with NRS IgG (1.42 ± 0.12-fold vs. nonstressed rats pretreated with NRS IgG; Fig. 3), and pretreatment with anti-Ucn2 IgG blocked immobilization stress-induced increase in miR-325-3p expression in the anterior pituitary (Fig. 3). There was a significant interaction between IgG injection and immobilization exposure ($F_{1,16}$ = 5.01, P = 0.040, n = 5).

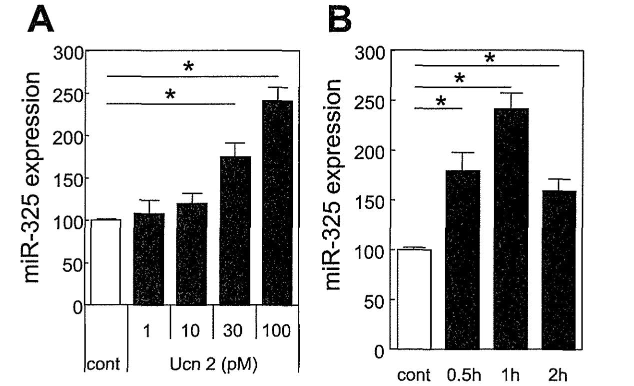

Fig. 2. Effects of urocortin 2 (Ucn2) on miR-325-3p expression in rat monolayer cultured anterior pituitary cells. *A*: miR-325-3p expression in anterior pituitary cells treated with Ucn2 at various concentrations ranging from 1 to 100 pM for 1 h. *B*: time course for miR-325-3p expression in anterior pituitary cells treated with 100 pM Ucn2. Levels are shown as % of control. Eight wells were used for each treatment. cont, control. Data shown are means ± SE. *P < 0.05 vs. control.

Overexpression and suppression of miR-325-3p affect intracellular contents and secretion of LH in vitro. miR-325-3p was overexpressed and suppressed by transfection with pBA-miR-325-3p and pDecoy-miR-325-3p, respectively (Fig. 4*A*). LH β-subunit mRNA expression was unaffected by miR-325-3p overexpression or knockdown (Fig. 4*B*). Overexpression of miR-325-3p significantly decreased intracellular LH (60.5 ± 4.7% of mock transfectants) and LH secretion (46.5 ± 11.4% of mock transfectants) (Fig. 4*C* and *E*). Ucn2 significantly decreased intracellular LH contents (60.4 ± 4.7% of control) and LH secretion (33.7 ± 8.9% of control) in pBA-mock transfectants, whereas there was no significant difference in intracellular contents and secretion of LH between control and Ucn2 treatment in pBA-miR-325-3p transfectants (Fig. 4, *C* and *E*). There was a significant interaction between transfectants and treatment ($F_{1,28}$ = 8.06, P = 0.008, n = 8) in intracellular LH content, but not in LH secretion. Knockdown of miR-325-3p expression by pDecoy vector blocked Ucn2-induced suppression of intracellular contents and secretion of LH (Fig. 4, *D* and *F*). There was no significant interaction

A

```
••••GCTAGCGCCCACCCACUAACUCCCCAUUCUUCU
GGAGCCAGCAGGUGUUCUAACCAUCCCUCCCAAUAAA
     |||||||                   |||||||
     GUCGUCC                   GUUAUUU
     rno-miR-370               rno-miR-325-3p

GGCUUUACAACUGCUCUAGA••••••
||||||
CCGAAA
rno-miR-742
```

B

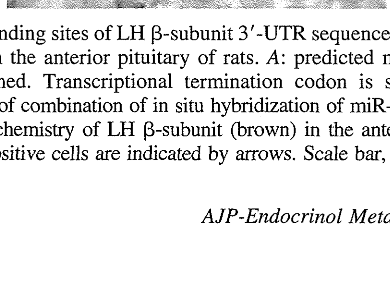

Fig. 1. miRNA binding sites of LH β-subunit 3′-UTR sequence and expression of miR-325-3p in the anterior pituitary of rats. *A*: predicted miRNA binding sites are underlined. Transcriptional termination codon is shown in bold. *B*: typical picture of combination of in situ hybridization of miR-325-3p (purple) and immunohistochemistry of LH β-subunit (brown) in the anterior pituitary is shown. Double-positive cells are indicated by arrows. Scale bar, 50 μm.

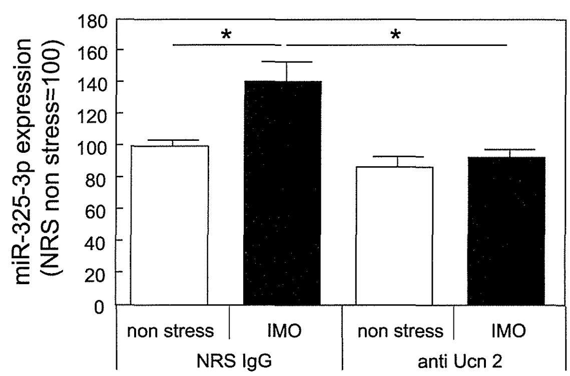

Fig. 3. Effect of anti-Ucn2 IgG pretreatment on miR-325-3p expression in the anterior pituitary of immobilization-stressed rats. NRS IgG, normal rabbit serum IgG-injected rats; anti-Ucn2, anti-Ucn2 IgG-injected rats; IMO, 90-min immobilization stress exposed group. miRNA expression levels are shown as % of that in NRS IgG-injected nonstressed controls. For each experimental group, n = 5. *P < 0.05 vs. nonstressed controls (nonstress).

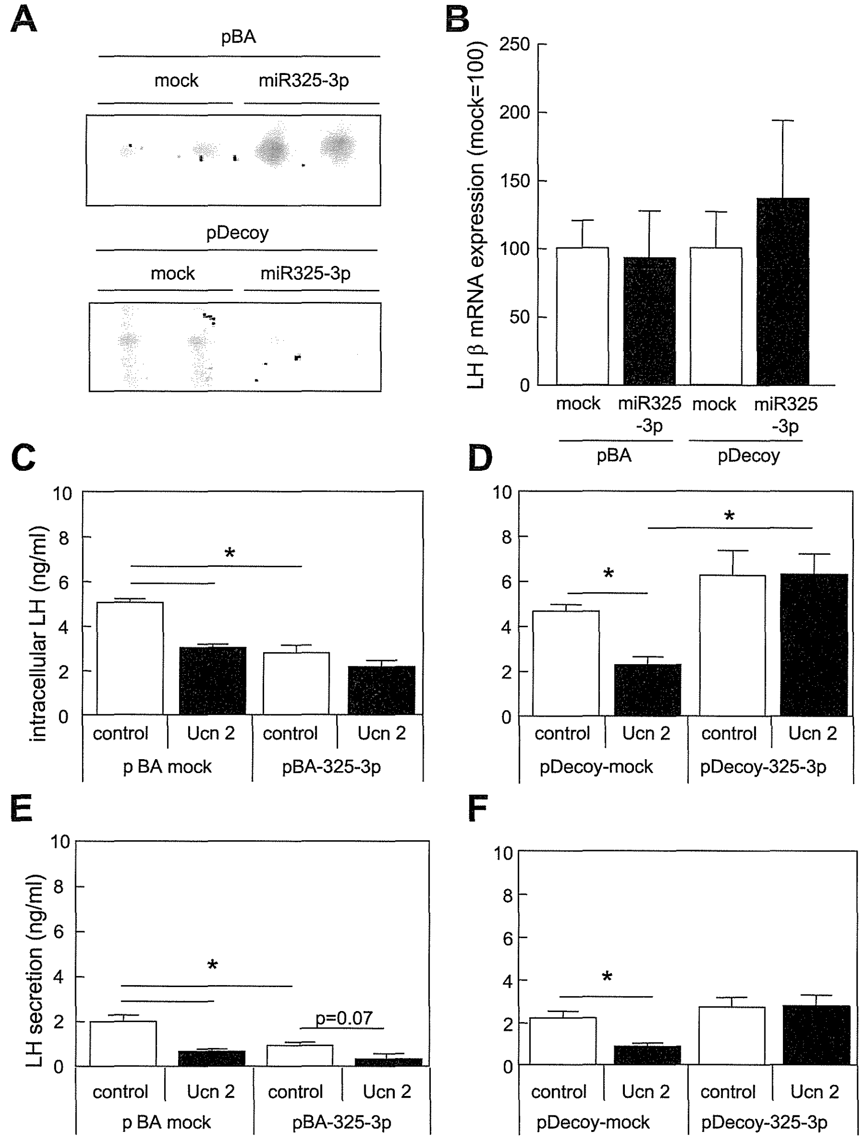

Fig. 4. Effects of overexpression or knockdown of miR-325-3p on LH secretion and contents and LH β-subunit mRNA expression in vitro. Cultured anterior pituitary cells were transfected with pBA-miR-325-3p, pBA-mock, pDecoy-miR-325-3p, or pDecoy-mock vectors. After 72 h, total RNA was extracted for Northern blot analyses of miR-325-3p expression (*A*). After 72 h, transfectant cells were each treated with 100 pM Ucn2 for 1 h and LH β-subunit mRNA expression (shown as %control) (*B*), and intracellular contents and secretion of LH (C and *E* for pBA-miR325–3p and D and *F* for pDecoy-miR-325-3p) were determined. Eight wells were used for each treatment. Data shown are means ± SE. *$P < 0.05$ vs. mock transfectants.

between transfectants and treatment in intracellular LH content and LH secretion.

LH β-subunit 3′-UTR activity assay. When intact LH β-subunit 3′-UTR-fused luciferase vector [pmir-Glo LHβ 3′-UTR (WT)] was cotransfected with miR-325-3p, its luciferase activity was significantly lower than that cotransfected with pBA-mock vector (75.9 ± 3.5% of mock transfectants; Fig. 5*B*). When the miR-325-3p binding site of LH β-subunit 3′-UTR was replaced with scramble mutation [pmir-Glo LHβ 3′-UTR (SC)], there was no difference in luciferase activity between pBA-325-3p coexpression and pBA-mock coexpression (Fig. 5*B*).

DISCUSSION

Our previous study has shown that Ucn2 suppresses LH secretion from monolayer cultured anterior pituitary cells of rats (23). In the present study, Ucn2 increased expression of miR-325-3p in the anterior pituitary cells of rats. The present study has also demonstrated that miR-325-3p overexpression decreases intracellular LH contents and suppresses basal LH secretion and LH β-subunit 3′-UTR activity, and that miR-325-3p knockdown blocks Ucn2-induced suppression of intracellular contents and secretion of LH. These results suggest that miRNA is involved in Ucn2-induced suppression of LH biosynthesis and secretion. Our previous study had also revealed that mRNA expression and secretion of Ucn2 in the pituitary are increased by CRF in vitro (20) and by immobilization stress in vivo (21), and that the increases of mRNA expression and secretion of Ucn2 in immobilization stress are blocked by anti-CRF IgG in vivo (21), suggesting that stress-induced CRF induces Ucn2 secretion. Furthermore, we showed that stress-induced suppression of LH secretion is blocked partially by anti-Ucn2 IgG in vivo (21). Considered together with these previous findings, the results of the present study suggest that stress-induced Ucn2 secretion causes an increase in miR-325-3p expression in the pituitary, which in turn suppresses LH β-subunit translation and secretion.

We tested the effect of intravenous administration of Ucn2 on LH secretion and miR-325-3p expression in the anterior pituitary of rats, and no significant changes in plasma LH or

A

pmir-Glo LHβ 3'UTR (WT)

• • • • GC**TAG**CGCCCACCCACUAACUCCCCAUUCUUCUGGAGCCAGCAGGUGU
UCUAACCAUCCCUCCCAAUAAAGGCUUUACAACUGCUCUAGA• • • • • •
| | | | | | |
GUUAUUU
rno-miR-325-3p

pmir-Glo LHβ 3'UTR (SC)

• • • • GC**TAG**CGCCCACCCACUAACUCCCCAUUCUUCUGGAGCCAGCAGGUGU
UCUAACCAUCCCUCC*acaaata*GGCUUUACAACUGCUCUAGA• • • • • •
GUUAUUU
rno-miR-325-3p

B

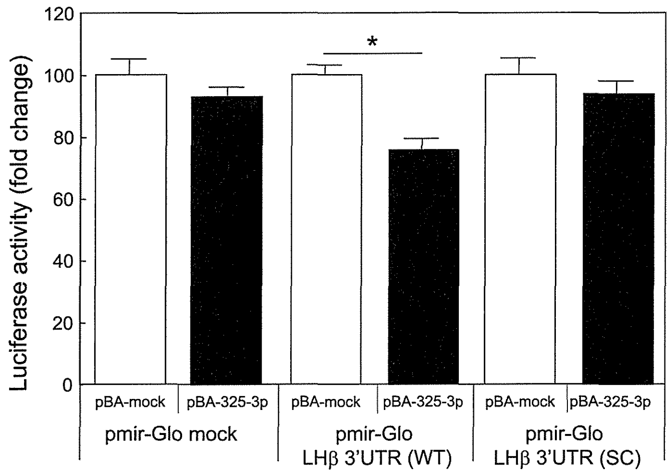

Fig. 5. Effects of overexpression of miR-325-3p on LH β-subunit 3′-UTR activity. *A*: sequences for LH β-subunit 3′-UTR [pmir-Glo LHβ 3′-UTR (WT) and pmir-Glo LHβ 3′-UTR (SC)], used in this study are shown. miR-325-3p binding site (underlined) is replaced with scramble mutation, which is not recognized by miR-325-3p. Transcriptional termination codon is shown in bold. *B*: HEK293 cells were cotransfected with pmir-Glo LHβ 3′-UTR (WT), pmir-Glo LHβ 3′-UTR (SC), or pmir-Glo mock plasmid and pBA-miR-325-3p or pBA-mock plasmid. After 72 h, firefly and *Renilla* luciferase activities were assayed, and transfection efficiency was obtained by calculating their ratios. Levels are shown as % of pBA-mock transfectants. Six wells were used for each assay. Data shown are means ± SE. *$P < 0.05$ vs. pBA-mock transfectants.

miR-325-3p expression levels in the anterior pituitary were induced by peripheral administration of Ucn2 at doses of 5 and 15 μg (data not shown). Since Ucn2 suppresses and a CRF-R2 antagonist increases LH secretion in the monolayer culture of rat anterior pituitary cells (23), these results suggest that factors that block or attenuate the inhibitory effect of Ucn2 on LH secretion may be present in the peripheral circulation. CRF-binding protein (CRF-BP), which shows an intermediate affinity to Ucn2, would be proposed as one of factors (12). There has been no study that shows CRF-BP in rat plasma; however, CRF-BP is likely to exist in peripheral blood of rats, because it is synthesized by adrenomedullary chromaffin cells (5) and kupffer cells (4) of rats, and CRF-BP is detected in human peripheral blood (9, 19). Therefore, Ucn2 administered intravenously may bind to CRF-BP during peripheral circulation before reaching the gonadotrophs of the pituitary and lose its inhibitory effect on gonadotrophs. In any case, the Ucn2 secreted by corticotrophs seems to act on gonadotrophs in a paracrine manner (23). Intracerebroventricular (icv) administration of Ucn2 reportedly suppresses LH secretion in rats, although the site of action of Ucn2 is unknown (17). Furthermore, icv administration of a selective CRF-R2 antagonist blocks restraint-, hypoglycemia-, or lipopolysaccharide-induced suppression of LH secretion in ovariectomized rats with estrogen replacement (16, 17). These findings suggest that CRF-R2 probably mediates stress-induced LH suppression at some site(s) other than the pituitary and that Ucn2 may play a role in the control of LH secretion under stress in the central nervous system.

Not only Ucn2 but also Ucn1, Ucn3, and CRF bind to CRF-R2. However, since there has been no report showing that the anterior pituitary cells express Ucn1 and Ucn3, it seems that they have no physiological role in the regulatory mechanism of LH secretion at the pituitary level. Furthermore, we have shown that CRF has no effect on LH secretion in the monolayer cultured anterior pituitary cells of rats (21). Therefore, CRF, an endogenous ligand to CRF-R1, does not seem to affect miR-325-3p expression, although 13% of gonadotrophs express CRF-R1 (31).

miR-325-3p is reportedly expressed in brain, spleen, and testis in rats (18). In addition to these tissues, we have found that miR-325-3p is expressed in the anterior pituitary and that it is, at least in part, expressed in LH cells in the present study. Therefore, the miR-325-3p expressed in LH cells seems to play a suppressive role in the regulatory mechanism of LH biosynthesis. Although pituitary cells other than LH cells also express miR-325-3p, the physiological significance of miR-325-3p in the cells is unknown. In general, one miRNA has various target genes, which may differ in each cell or tissue (14). Actually, miR-325-3p has more than 1,000 target genes detected using the Targetscan database. Further studies are needed to clarify the functions of miR-325-3p in other pituitary cells.

The present study has shown that overexpression and knockdown of miR-325-3p did not affect LH β-subunit mRNA expression, although the intracellular content and secretion of Ucn2 were influenced, suggesting that miR-325-3p inhibits translation but not transcription. These results are consistent with our previous in vitro study showing that Ucn2 suppresses LH secretion without changing LH β-subunit mRNA expression. By contrast, immobilization stress suppresses not only LH secretion but also LH β-subunit mRNA expression, and these changes are completely reversed by pretreatment with anti-CRF IgG, whereas anti-Ucn2 IgG significantly but partially blocked the immobilization-induced changes (21). Taking these findings into consideration, it seems that some factor other than the Ucn2/miR-325-3p system, which is induced by CRF, is involved in immobilization stress-induced suppression of LH β-subunit mRNA expression.

The human genome may encode thousands of miRNAs, which are abundantly expressed in many human cell types and may target about 60% of genes (3). These miRNAs target the 3′-UTR of mRNAs to inhibit translation. Recent studies have revealed that miRNAs have many physiological roles in endocrine and metabolic systems. Progesterone receptor translation and casein secretion are inhibited by miR-126-3p in mouse mammary epithelial cells (6). Toll-like receptor 4 is suppressed by miR-146a, and miR-146a reduces intracellular LDL cholesterol and secretions of IL-6, IL-8, chemokine ligand 2, and MMP-9 by inhibiting the toll-like receptor 4 signaling pathway (33). Since high glucose concentrations increase miR-410, miR-200a, and miR-130a expression, these may be involved in glucose-stimulated insulin secretion in MIN6 cells (11). Concerning the hypothalamic-pituitary-gonadal axis, it has been shown that FSH downregulates miR-29a and miR-30d expression, which are involved in steroidogenic signaling pathways in cultured granulosa cells (34). Furthermore, it has been reported that GnRH increases miR-132 and miR-212 expression and that these are implicated in GnRH-stimulated cellular biochemical metabolic responses in LβT2 cells (35). However, the physiological role of miRNAs in pituitary hormone secretion has not been reported. The current study provides new insight into understanding the function of miRNAs in regulating pituitary hormone biosynthesis.

Although miRNA transcription is controlled by RNA polymerase II or III and primary miRNA is processed in the nucleus (2, 7, 15), little is known about the signaling pathways that control its expression. It was reported that protein kinase A (PKA) affects the Wnt signaling pathway and that inhibition of PKA-induced Wnt-β catenin signaling is mediated by miRNA expression (13). We previously demonstrated that Ucn2 activates PKA and MAPK in PC12 cells (22). Unfortunately, H-89 and Rp-cAMPs, both PKA inhibitors, failed to block Ucn2-induced miR-325-3p expression, and miR-325-3p expression was unaffected by forskolin, a PKA activator (data not shown). Further studies are needed to clarify other intracellular signaling pathways leading to Ucn2-induced increases in miR-325-3p expression.

In summary, the present study suggests that miR-325-3p is involved in stress-induced suppression of LH secretion and that Ucn2 plays a role in increasing the expression of miR-325-3p. This is a newly identified pathway underlying regulation of LH secretion. These results may increase our understanding of the molecular mechanisms involved in development of stress-induced gonadal dysfunction.

ACKNOWLEDGMENTS

We are grateful to Shino Inada and Mitsue Iketani for excellent technical assistance.

GRANTS

This study was supported in part by grants from Research on Measures for Intractable Diseases, Health and Labor Sciences Research Grants from the Ministry of Health, Labor and Welfare and "Research Core" Project for Private University, and a Matching Fund Subsidy from the Ministry of Education, Science and Culture of Japan.

DISCLOSURES

No conflicts of interest, financial or otherwise, are declared by the author(s).

AUTHOR CONTRIBUTIONS

Author contributions: T.N. conception and design of research; T.N. and A.M. performed experiments; T.N. analyzed data; T.N. prepared figures; T.N. drafted manuscript; T.N. approved final version of manuscript; T.S. interpreted results of experiments; T.S. edited and revised manuscript.

REFERENCES

1. **Arai K, Ohata H, Shibasaki T.** Non-peptidic corticotropin-releasing hormone receptor type 1 antagonist reverses restraint stress-induced shortening of sodium pentobarbital-induced sleeping time of rats: evidence that an increase in arousal induced by stress is mediated through CRH receptor type 1. *Neurosci Lett* 255: 103–106, 1998.
2. **Borchert GM, Lanier W, Davidson BL.** RNA polymerase III transcribes human microRNAs. *Nat Struct Mol Biol* 13: 1097–1101, 2006.
3. **Carthew RW, Sontheimer EJ.** Origins and Mechanisms of miRNAs and siRNAs. *Cell* 136: 642–655, 2009.
4. **Charalampopoulos I, Androulidaki A, Minas V, Chatzaki E, Tsatsanis C, Notas G, Xidakis C, Kolios G, Kouroumalis E, Margioris AN, Gravanis A.** Neuropeptide urocortin and its receptors are expressed in rat Kupffer cells. *Neuroendocrinology* 84: 49–57, 2006.
5. **Chatzaki E, Margioris AN, Gravanis A.** Expression and regulation of corticotropin-releasing hormone binding protein (CRH-BP) in rat adrenals. *J Neurochem* 80: 81–90, 2002.
6. **Cui W, Li Q, Feng L, Ding W.** MiR-126-3p regulates progesterone receptors and involves development and lactation of mouse mammary gland. *Mol Cell Biochem* 355: 17–25, 2011.
7. **Dieci G, Fiorino G, Castelnuovo M, Teichmann M, Pagano A.** The expanding RNA polymerase III transcriptome. *Trends Genet* 23: 614–622, 2007.
8. **Findlay JK, Drummond AE, Dyson M, Baillie AJ, Robertson DM, Ethier JF.** Production and actions of inhibin and activin during folliculogenesis in the rat. *Mol Cell Endocrinol* 180: 139–144, 2001.
9. **Florio P, Imperatore A, Sanseverino F, Torricelli M, Reis FM, Lowry PJ, Petraglia F.** The measurement of maternal plasma corticotropin-releasing factor (CRF) and CRF-binding protein improves the early prediction of preeclampsia. *J Clin Endocrinol Metab* 89: 4673–4677, 2004.
10. **Gharib SD, Wierman ME, Badger TM, Chin WW.** Sex steroid hormone regulation of follicle-stimulating hormone subunit messenger ribonucleic acid (mRNA) levels in the rat. *J Clin Invest* 80: 294–299, 1987.
11. **Hennessy E, Clynes M, Jeppesen PB, O'Driscoll L.** Identification of microRNAs with a role in glucose stimulated insulin secretion by expression profiling of MIN6 cells. *Biochem Biophys Res Commun* 396: 457–462, 2010.
12. **Huising MO, Vaughan JM, Shah SH, Grillot KL, Donaldson CJ, Rivier J, Flik G, Vale WW.** Residues of corticotropin releasing factor-binding protein (CRF-BP) that selectively abrogate binding to CRF but not to urocortin 1. *J Biol Chem* 283: 8902–8912, 2008.
13. **Iliopoulos D, Bimpaki EI, Nesterova M, Stratakis CA.** MicroRNA signature of primary pigmented nodular adrenocortical disease: clinical correlations and regulation of Wnt signaling. *Cancer Res* 69: 3278–3282, 2009.
14. **John B, Enright AJ, Aravin A, Tuschl T, Sander C, Marks DS.** Human MicroRNA targets. *PLoS Biol* 2: e363, 2004.
15. **Lee Y, Kim M, Han J, Yeom KH, Lee S, Baek SH, Kim VN.** MicroRNA genes are transcribed by RNA polymerase II. *EMBO J* 23: 4051–4060, 2004.
16. **Li XF, Bowe JE, Kinsey-Jones JS, Brain SD, Lightman SL, O'Byrne KT.** Differential role of corticotrophin-releasing factor receptor types 1 and 2 in stress-induced suppression of pulsatile luteinising hormone secretion in the female rat. *J Neuroendocrinol* 18: 602–610, 2006.
17. **Li XF, Bowe JE, Lightman SL, O'Byrne KT.** Role of corticotropin-releasing factor receptor-2 in stress-induced suppression of pulsatile luteinizing hormone secretion in the rat. *Endocrinology* 146: 318–322, 2005.
18. **Linsen SE, de Wit E, de Bruijn E, Cuppen E.** Small RNA expression and strain specificity in the rat. *BMC Genomics* 11: 249, 2010.
19. **Lowry PJ.** Corticotropin-releasing factor and its binding protein in human plasma. *Ciba Found Symp* 172: 108–115; discussion 115–128, 1993.
20. **Nemoto T, Iwasaki-Sekino A, Yamauchi N, Shibasaki T.** Regulation of the expression and secretion of urocortin 2 in rat pituitary. *J Endocrinol* 192: 443–452, 2007.
21. **Nemoto T, Iwasaki-Sekino A, Yamauchi N, Shibasaki T.** Role of urocortin 2 secreted by the pituitary in the stress-induced suppression of luteinizing hormone secretion in rats. *Am J Physiol Endocrinol Metab* 299: E567–E575, 2010.
22. **Nemoto T, Mano-Otagiri A, Shibasaki T.** Urocortin 2 induces tyrosine hydroxylase phosphorylation in PC12 cells. *Biochem Biophys Res Commun* 330: 821–831, 2005.
23. **Nemoto T, Yamauchi N, Shibasaki T.** Novel action of pituitary urocortin 2 in the regulation of expression and secretion of gonadotropins. *J Endocrinol* 201: 105–114, 2009.
24. **Nolan T, Hands RE, Bustin SA.** Quantification of mRNA using real-time RT-PCR. *Nat Protoc* 1: 1559–1582, 2006.
25. **Pakarinen P, Huhtaniemi I.** Gonadal and sex steroid feedback regulation of gonadotrophin mRNA levels and secretion in neonatal male and female rats. *J Mol Endocrinol* 3: 139–144, 1989.

26. **Pierce JG, Parsons TF.** Glycoprotein hormones: structure and function. *Annu Rev Biochem* 50: 465–495, 1981.
27. **Reyes TM, Lewis K, Perrin MH, Kunitake KS, Vaughan J, Arias CA, Hogenesch JB, Gulyas J, Rivier J, Vale WW, Sawchenko PE.** Urocortin II: a member of the corticotropin-releasing factor (CRF) neuropeptide family that is selectively bound by type 2 CRF receptors. *Proc Natl Acad Sci USA* 98: 2843–2848, 2001.
28. **Rivest S, Rivier C.** Central mechanisms and sites of action involved in the inhibitory effects of CRF and cytokines on LHRH neuronal activity. *Ann NY Acad Sci* 697: 117–141, 1993.
29. **Rivier C, Rivest S.** Effect of stress on the activity of the hypothalamic-pituitary-gonadal axis: peripheral and central mechanisms. *Biol Reprod* 45: 523–532, 1991.
30. **Tran U, Zakin L, Schweickert A, Agrawal R, Doger R, Blum M, De Robertis EM, Wessely O.** The RNA-binding protein bicaudal C regulates polycystin 2 in the kidney by antagonizing miR-17 activity. *Development* 137: 1107–1116, 2010.
31. **Westphal NJ, Evans RT, Seasholtz AF.** Novel expression of type 1 corticotropin-releasing hormone receptor in multiple endocrine cell types in the murine anterior pituitary. *Endocrinology* 150: 260–267, 2009.
32. **Yamauchi N, Otagiri A, Nemoto T, Sekino A, Oono H, Kato I, Yanaihara C, Shibasaki T.** Distribution of urocortin 2 in various tissues of the rat. *J Neuroendocrinol* 17: 656–663, 2005.
33. **Yang K, He YS, Wang XQ, Lu L, Chen QJ, Liu J, Sun Z, Shen WF.** MiR-146a inhibits oxidized low-density lipoprotein-induced lipid accumulation and inflammatory response via targeting toll-like receptor 4. *FEBS Lett* 585: 854–860, 2011.
34. **Yao N, Yang BQ, Liu Y, Tan XY, Lu CL, Yuan XH, Ma X.** Follicle-stimulating hormone regulation of microRNA expression on progesterone production in cultured rat granulosa cells. *Endocrine* 38: 158–166, 2010.
35. **Yuen T, Ruf F, Chu T, Sealfon SC.** Microtranscriptome regulation by gonadotropin-releasing hormone. *Mol Cell Endocrinol* 302: 12–17, 2009.

Am J Physiol Endocrinol Metab 302: E924–E931, 2012.
First published January 24, 2012; doi:10.1152/ajpendo.00198.2011.

Amylin improves the effect of leptin on insulin sensitivity in leptin-resistant diet-induced obese mice

Toru Kusakabe,[1] Ken Ebihara,[1,2] Takeru Sakai,[1] Licht Miyamoto,[1] Daisuke Aotani,[1] Yuji Yamamoto,[1] Sachiko Yamamoto-Kataoka,[1] Megumi Aizawa-Abe,[2] Junji Fujikura,[1] Kiminori Hosoda,[1,2] and Kazuwa Nakao[1]

[1]*Department of Medicine and Clinical Science, Kyoto University Graduate School of Medicine; and* [2]*Translational Research Center, Kyoto University Hospital, Kyoto, Japan*

Submitted 25 April 2011; accepted in final form 19 January 2012

Kusakabe T, Ebihara K, Sakai T, Miyamoto L, Aotani D, Yamamoto Y, Yamamoto-Kataoka S, Aizawa-Abe M, Fujikura J, Hosoda K, Nakao K. Amylin improves the effect of leptin on insulin sensitivity in leptin-resistant diet-induced obese mice. *Am J Physiol Endocrinol Metab* 302: E924–E931, 2012. First published January 24, 2012; doi:10.1152/ajpendo.00198.2011.—Leptin enhances insulin sensitivity in addition to reducing food intake and body weight. Recently, amylin, a pancreatic β-cell-derived hormone, was shown to restore a weight-reducing effect of leptin in leptin-resistant diet-induced obesity. However, whether amylin improves the effect of leptin on insulin sensitivity in diet-induced obesity is unclear. Diet-induced obese (DIO) mice were infused with either saline (S), leptin (L; 500 $\mu g \cdot kg^{-1} \cdot day^{-1}$), amylin (A; 100 $\mu g \cdot kg^{-1} \cdot day^{-1}$), or leptin plus amylin (L/A) for 14 days using osmotic minipumps. Food intake, body weight, metabolic parameters, tissue triglyceride content, and AMP-activated protein kinase (AMPK) activity were examined. Pair-feeding and weight-matched calorie restriction experiments were performed to assess the influence of food intake and body weight reduction. Continuous L/A coadministration significantly reduced food intake, increased energy expenditure, and reduced body weight, whereas administration of L or A alone had no effects. L/A coadministration did not affect blood glucose levels during ad libitum feeding but decreased plasma insulin levels significantly (by 48%), suggesting the enhancement of insulin sensitivity. Insulin tolerance test actually showed the increased effect of insulin in L/A-treated mice. In addition, L/A coadministration significantly decreased tissue triglyceride content and increased AMPKα2 activity in skeletal muscle (by 67%). L/A coadministration enhanced insulin sensitivity more than pair-feeding and weight-matched calorie restriction. In conclusion, this study demonstrates the beneficial effect of L/A coadministration on glucose and lipid metabolism in DIO mice, indicating the possible clinical usefulness of L/A coadministration as a new antidiabetic treatment in obesity-associated diabetes.

obesity; diabetes; adenosine 5′-monophosphate-activated protein kinase

LEPTIN, AN ADIPOCYTE-DERIVED HORMONE, has a weight-reducing effect accompanied by reduction in food intake and increase in energy expenditure (11, 13). In general, in rodent models of diet-induced obesity and obese human, although leptin levels rise proportionally with adiposity (16, 23), the increased leptin fails to suppress the progression of obesity. Moreover, even high pharmacological doses of leptin have demonstrated only marginal, if any, effects on body weight in diet-induced obese (DIO) rodents and obese humans (8, 15). This leptin ineffectiveness is called leptin resistance.

Recently, it was shown that amylin, a pancreatic β-cell-derived hormone (4), restored a weight-reducing effect of leptin and that leptin/amylin coadministration effectively reduced body weight in DIO rats (34). Moreover, in overweight/obese humans, coadministration of the amylin analog pramlintide and the leptin analog metreleptin induced significantly greater weight loss than either pramlintide or metreleptin alone (32, 34).

Besides the weight-reducing effect, leptin has a wide range of effects, including an antidiabetic effect. We previously generated transgenic skinny mice (LepTg) overexpressing leptin under the control of the liver-specific human serum amyloid P component promoter, whose plasma leptin levels are elevated compared with those of obese human individuals (30). LepTg mice showed increased glucose metabolism. In LepTg mice, we have demonstrated that leptin increases insulin sensitivity with augmentation of liver and skeletal muscle insulin receptor signaling (30). In addition, LepTg mice had reduced tissue triglyceride contents along with increased energy expenditure through activation of AMP-activated protein kinase (AMPK) (37, 38), a key enzyme that mediates the effect of leptin on fatty acid β-oxidation in skeletal muscle (24).

Given the antidiabetic effect of leptin, we have demonstrated that leptin could be an antidiabetic drug for various types of diabetes, such as lipoatrophic, insulin-deficient, and type 2 diabetes, using animal models (7, 18, 25, 28, 29). In addition, we and others confirmed that leptin treatment effectively reduces food intake and improves insulin sensitivity, hyperglycemia, hypertriglyceridemia, and fatty liver in patients with lipoatrophic diabetes (2, 5, 6, 31). However, in DIO rodents and obese humans, the effect of leptin on insulin sensitivity is also attenuated because of leptin resistance (18).

Evidence indicating that leptin can stimulate insulin sensitivity independently of food intake and body weight reduction via central mechanisms has accumulated (9, 14, 17, 27). Amylin also activates multiple central nervous system regions to regulate both energy and glucose homeostasis (19, 21, 22). Therefore, it is possible that leptin and amylin interact with each other in the regulation of glucose metabolism. However, whether amylin improves the effect of leptin on insulin sensitivity in leptin-resistant obese subjects is unclear.

In this study, we demonstrated that leptin/amylin coadministration, unlike administration of leptin or amylin alone, enhances insulin sensitivity in leptin-resistant DIO mice in addition to reducing body weight accompanied by reduction in food intake and increase in energy expenditure, indicating the pos-

Address for reprint requests and other correspondence: K. Ebihara, Dept. of Medicine and Clinical Science, Kyoto University Graduate School of Medicine, 54 Shogoin Kawahara-cho, Sakyo-ku, Kyoto 606-8507, Japan (e-mail: kebihara@kuhp.kyoto-u.ac.jp).

sible clinical usefulness of leptin/amylin coadministration as a new antidiabetic treatment in obesity-associated diabetes.

MATERIALS AND METHODS

Experimental animals. Eight-week-old male C57BL/6J mice were purchased from Japan SLC, Shizuoka, Japan. The mice were caged individually and kept under a 12:12-h light-dark cycle (lights on at 0900). The mice were fed a high-fat diet (D12451, 45% of energy as fat; Research Diets, New Brunswick, NJ) for 5 wk, with free access to water (termed DIO mice), before experiments. Body weight of DIO mice before experiments was significantly heavier than that of control mice fed a standard diet (NMF, 13% of energy as fat; Oriental Yeast, Tokyo, Japan) (32.6 ± 0.5 vs. 26.9 ± 0.4 g, $P < 0.01$). Metabolic characteristics of control and DIO mice are summarized in Table 1. The result of an insulin tolerance test (ITT) showed that DIO mice were insulin resistant compared with control mice. Animal care and all experiments were conducted in accordance with the Guidelines for Animal Experiments of Kyoto University and were approved by the Animal Research Committee, Graduate School of Medicine, Kyoto University.

Leptin and/or amylin infusion experiments. DIO mice were divided into four treatment groups [saline (S), leptin (L), amylin (A), and leptin plus amylin (L/A)] to be counterbalanced for starting body weight and blood glucose level. On *day 0*, all mice were implanted subcutaneously in the midscapular region with two osmotic minipumps (Alzet model 2002; Alza, Palo Alto, CA) containing either saline, leptin (500 $\mu g \cdot kg^{-1} \cdot day^{-1}$; Amgen, Thousand Oaks, CA), or amylin (100 $\mu g \cdot kg^{-1} \cdot day^{-1}$; Bachem, Torrance, CA). High-fat diet feeding was continued during the experiment.

Body weight and food intake. Body weight was measured on *days 0, 5*, and *10*. Daily food intake was measured before and during the leptin and/or amylin infusion experiment.

Indirect calorimetry. Measurement of oxygen consumption ($\dot{V}O_2$) and carbon dioxide production ($\dot{V}CO_2$) was performed over a period of 48 h, after >72 h of acclimation, using an Oxymax indirect calorimeter (Columbus Instruments, Columbus, OH) on *days 4* and *5* (n = 4/group) for S, L, A, and L/A-treated mice. Respiratory exchange ratio [ratio of CO_2 production to O_2 ($\dot{V}CO_2/O_2$)], which indicates the relative contribution of fat and carbohydrate oxidation to overall metabolism, was calculated and averaged across the 48-h measurement session.

Metabolic variables. Blood was obtained from nonfasted mice between 1500 and 1700 at the end of the experiment. Blood glucose levels were measured by the glucose oxidase method using a reflectance glucometer (MS-GR102; Terumo, Tokyo, Japan). Plasma insulin levels were measured by enzyme immunoassay with an Insulin-EIA kit (Morinaga, Tokyo, Japan). Plasma glucagon levels were measured by enzyme immunoassay with a Glucagon-EIA kit (Yanaihara, Shizuoka, Japan). Plasma leptin levels were measured by an ELISA kit for mouse leptin (Millipore, Billerica, MA). Plasma amylin levels were measured by enzyme immunoassay using a mouse Amylin-EIA kit (Phoenix Pharmaceuticals, Burlingame, CA).

ITT. An ITT was performed on *day 10*. For the ITT, after a 4-h fast, mice were injected with 0.8 mU/g ip human regular insulin (Humulin R; Eli Lilly Japan, Kobe, Japan). Blood was sampled from the tail vein before and 30, 60, and 120 min after the insulin injection. Blood glucose levels were determined as described above. The area under the curve (AUC) during the ITT was calculated in each mouse.

Liver weight and tissue triglyceride content. Liver weight was measured at the end of the experiment. Liver and skeletal muscle triglyceride content were measured as described previously (18). Liver and gastrocnemius muscle were isolated at the end of the experiment and immediately frozen in liquid nitrogen, and lipids were extracted with isopropyl alcohol-heptane (1:1, vol/vol). After the solvent was evaporated, the lipids were resuspended in 99.5% (vol/vol) ethanol, and the triglyceride content was measured using the Triglyceride E-test Wako kit (Wako Pure Chemicals, Osaka, Japan).

Isoform-specific AMPK activity. AMPK activity was determined as described previously (18). Soleus muscles were isolated at the end of the experiment and immediately frozen in liquid nitrogen. To measure isoform-specific AMPKα1 and -α2 activity in soleus muscle, AMPK was immunoprecipitated from muscle lysates (200 μg of protein) with specific antibodies against the α_1- and α_2-subunits (Upstate Cell Signaling Solutions, Lake Placid, NY) bound to Protein A-Sepharose beads, and the kinase activity of the immunoprecipitates was measured using "SAMS" peptide and [γ-^{32}P]ATP.

Pair-feeding and weight-matched calorie restriction experiments. Pair-feeding experiments were performed to assess the influence of food intake reduction. In this experiment, DIO mice (mean body weight 31.2 ± 0.4 g) were divided into three treatment groups [S, saline + pair-fed L/A-treated mice (PF), and L/A] to be counterbalanced for starting body weight and blood glucose level. Saline, leptin, and amylin were infused using two osmotic minipumps, as described above. Pair-fed mice were fed the same amount of food consumed by L/A-treated mice on the previous day at the end of light phase once for 14 days. Body weight was measured on *days 0* and *10*. Weight-matched calorie restriction experiments were performed to assess the influence of body weight reduction. In this experiment, the food consumption of DIO mice (mean body weight 31.7 ± 0.5 g) was restricted to match their body weight to those of L/A-treated mice (weight-matched DIO mice, termed CR mice). CR mice were fed the ~70% amount of food consumed by S-treated mice on the previous day at the end of light phase at once for 14 days. An ITT was performed on *day 10* of these experiments. Liver and gastrocnemius muscle were obtained for triglyceride content measurements at the end of these experiments.

Statistical analyses. Data are expressed as means ± SE. Comparison between or among groups was by Student's *t*-test or ANOVA with Fisher's protected least significant difference test. $P < 0.05$ was considered statistically significant.

Table 1. *Metabolic characteristics of control and DIO mice*

Variable	Control (n = 6)	DIO (n = 9)
Blood glucose, mg/dl	142.4 ± 5.4	160.4 ± 6.6
Plasma insulin, pg/ml	466.9 ± 99.1	535.0 ± 87.6
AUC in ITT, %/min × 100	77.3 ± 10.5	102.5 ± 5.5*
Liver TG content, mg/g tissue	9.8 ± 0.8	23.6 ± 2.4**
Skeletal muscle TG content, mg/g tissue	5.2 ± 0.7	5.6 ± 1.1

Values are means ± SE. DIO, diet-induced obese; AUC, area under the curve; ITT, insulin tolerance test; TG, triglyceride. Blood glucose, plasma insulin, liver TG content, and skeletal muscle TG content were measured in saline-treated control and DIO mice at the end of the experiment. Blood samples were obtained during ad libitum feeding. AUC in ITT was measured on *day 10*. *$P < 0.05$ and **$P < 0.01$ vs. control mice.

RESULTS

Effect of leptin and/or amylin on food intake, body weight, and energy expenditure in DIO mice. Leptin and amylin were administered for 14 days in DIO mice, using osmotic minipumps. Plasma leptin and amylin levels at the end of the experiment were shown in Table 2. Administration of leptin (500 $\mu g \cdot g^{-1} \cdot day^{-1}$) was adequately effective in control mice fed a standard diet, as shown in our previous report (18), but it had no significant effect on food intake or body weight in DIO mice (Fig. 1, *A* and *B*), indicating that these DIO mice were in the leptin-resistant state. Administration of amylin (100 $\mu g \cdot g^{-1} \cdot day^{-1}$) had no effect on food intake or body weight in mice fed a standard diet (data not shown) or DIO mice (Fig. 1, *A* and *B*). However, L/A coadminis-